JOURNAL OF BACTERIOLOGY, Dec. 2002, p. 7025–7041 Vol. 184, No. 24
0021-9193/02/$04.00+0 DOI: 10.1128/JB.184.24.7025–7041.2002


# Ultrastructural Analysis of Differentiation in *Legionella pneumophila*

Gary Faulkner[1] and Rafael A. Garduño[1,2]*

*Department of Microbiology and Immunology[1] and Department of Medicine, Division of Infectious Diseases,[2] Faculty of Medicine, Dalhousie University, Halifax, Nova Scotia B3H-4H7, Canada*

Received 14 May 2002/Accepted 19 September 2002

***Legionella pneumophila*** **is an adaptive pathogen that replicates in the intracellular environment of fundamentally divergent hosts (freshwater protozoa and mammalian cells) and is capable of surviving long periods of starvation in water when between hosts. Physiological adaptation to these quite diverse environments seems to be accompanied by morphological changes (Garduño et al., p. 82-85, *in* Marre et al., ed., *Legionella*, 2001) and conceivably involves developmental differentiation. In following the fine-structural pathway of *L. pneumophila* through both in vitro and in vivo growth cycles, we have now discovered that this bacterium displays an unprecedented number of morphological forms, as revealed in ultrathin sections and freeze-fracture replicas for transmission electron microscopy. Many of the forms were identified by the obvious ultrastructural properties of their cell envelope, which included changes in the relative opaqueness of membrane leaflets, vesiculation, and/or profuse invagination of the inner membrane. These changes were best documented with image analysis software to obtain intensity tracings of the envelope in cross sections. Also prominent were changes in the distribution of intramembranous particles (clearly revealed in replicas of freeze-fractured specimens) and the formation of cytoplasmic inclusions. Our results confirm that *L. pneumophila* is a highly pleomorphic bacterium and clarify some early observations suggesting sporogenic differentiation in *L. pneumophila*. Since morphological changes occurred in a conserved sequence within the growth cycle, our results also provide strong evidence for the existence of a developmental cycle in *L. pneumophila* that is likely accompanied by profound physiological alterations and stage-specific patterns of gene expression.**

*Legionella pneumophila* is a gram-negative bacterial pathogen that has evolved to replicate in the intracellular compartment of freshwater amoebae (3, 9, 21). Accidentally, *L. pneumophila* infects the alveolar macrophages of susceptible humans and causes the atypical pneumonia known as Legionnaires' disease. The intracellular environment not only represents a survival haven for *L. pneumophila* but also seems to be essential for replication, implying that, in spite of its ability to grow in artificial media in the laboratory, *L. pneumophila* is a natural obligate intracellular pathogen (3, 20, 21). After egressing from a wasted host, extracellular *L. pneumophila* survives extended periods of starvation in fresh water (45, 58, 60), perhaps in a nonculturable form (61), until it finds a new protozoan host.

Central to the pathogenesis and ecology of obligate intracellular bacterial pathogens with an extracellular phase (well-studied examples being *Chlamydia* and *Coxiella* spp.) is the ability to differentiate into various forms within a developmental cycle (35, 36, 46, 48, 49, 57). Typically, after or during their intracellular replication, these pathogens differentiate into a highly infectious and environmentally resilient form that survives extracellularly. This combination of traits improves the odds of finding and infecting new hosts. Upon gaining access to the intracellular environment of a new host, differentiation into a replicative (and delicate) intracellular form closes the cycle.

We have presented experimental evidence elsewhere (27) to suggest that *L. pneumophila* differentiates intracellularly into a distinct mature intracellular form (MIF) that is infectious and environmentally resilient and has a low respiration rate. In addition, we have observed that MIFs give rise to morphologically distinct intermediates when placed in nutrient-rich laboratory media, which in turn give rise to replicative forms that display the morphology typical of gram-negative bacteria (26). Finally, the fact that MIFs alternate with replicative forms in each growth cycle strongly suggests the presence of a developmental cycle in *L. pneumophila* (26, 27).

The intracellular events that follow the invasion of a host cell by *L. pneumophila* and lead to the establishment of a specialized intracellular compartment known as the replicative vacuole have been well described at the ultrastructural level (1, 10, 29, 39, 51). Regardless of the type of host cell infected (an amoeba, human macrophage, or other mammalian cell), the sequence of intracellular morphological events is rather conserved and involves the alteration of organelle trafficking, a process largely (albeit not exclusively [40]) mediated by the Dot/Icm system of *L. pneumophila* (6, 8, 11, 56). First, the legionella-containing vacuole associates with numerous vesicles and mitochondria but does not apparently fuse with lysosomes or other components of the endocytic pathway. Then, the vacuole associates with ribosomes and apparently fuses with the endoplasmic reticulum, an event that somehow correlates with the onset of bacterial replication (1, 63, 64). The vacuole-endoplasmic reticulum then begins to acquire an unusually complex configuration and expands throughout the cytoplasm of the infected cell to accommodate the increasing numbers of replicating bacteria (1, 29, 39, 51). This replicative vacuole remains associated with ribosomes and mitochondria. In the late stages of the infection, as the host cell is wasted, the legionella-containing vacuole matures into a more spherical

* Corresponding author. Mailing address: Department of Microbiology & Immunology, Sir Charles Tupper Medical Building, 7th floor, Dalhousie University, 5859 University Avenue, Halifax, Nova Scotia, Canada B3H-4H7. Phone: (902) 494-6575. Fax: (902) 494-5125. E-mail: rafael.garduno@dal.ca.

compartment that loses its association with host cell organelles (1, 29, 51). Finally, the bacteria contained in these mature vacuoles are released via bacterially mediated lysis of the vacuolar membrane (5, 24, 47).

With the aforementioned well-described host cell events of the *L. pneumophila* infection, particularly as they occur in HeLa cells (29), we have documented and timed previously unrecognized morphological changes that occur during the bacterial intracellular growth cycle. Also, we have followed the morphological changes that *L. pneumophila* experiences when grown in vitro. Here we report that *L. pneumophila* has numerous morphologically distinct forms and clearly displays a stage-specific morphological cycle that is compatible with the existence of a developmental cycle.

## MATERIALS AND METHODS

**Bacterial strains.** *L. pneumophila* Philadelphia-1, Lp1-SVir, is a spontaneous streptomycin-resistant virulent strain obtained from P. S. Hoffman (Dalhousie University, Halifax, Canada) (37). A local clinical isolate from Halifax, Canada, *L. pneumophila* Olda strain 2064 (18), was also used. Strains were kept as frozen stocks (−70°C) routinely made from infected cultures of HeLa cells. Frozen stocks were grown on buffered charcoal yeast extract agar (BCYE) (52) for 3 to 5 days at 37°C in a humid incubator and used immediately to infect HeLa cells. Some cultures were grown in vitro in buffered yeast extract broth (BYE). BYE was based on the formulation of BCYE, but charcoal and agar were omitted.

**HeLa cells and infection protocols.** HeLa cells were routinely grown in 100-ml spinner bottles in Dulbecco's modified Eagle's medium (DMEM, high-glucose formulation) completed with 10% newborn calf serum and an antibiotic-antimycotic mixture (all from Gibco Laboratories). Before infection with *L. pneumophila*, HeLa cells were allowed to attach and spread on tissue culture flasks or multiwell plates (all from Falcon Plastics, Becton Dickinson). HeLa cells in 25- and 75-$cm^2$ cell culture flasks were typically infected with 1 or 2 ml, respectively, of a bacterial cell suspension of $10^9$ bacteria/ml (one optical density unit at 620 nm). After an overnight incubation, monolayers were washed twice with Earle's salt solution to eliminate free bacteria and cells, and fresh DMEM containing 100 μg of gentamicin per ml was added for 90 min. Monolayers were then washed twice with Earle's salt solution to remove the medium with gentamicin, and fresh DMEM with serum but no antibiotics was added.

**Purification of intracellular forms.** Replicative and mature intracellular bacteria were purified from infected HeLa cells in a self-generated, continuous-density gradient of Percoll by a modification of a previously reported method (29). In the modified method, the use of Triton X-100 to lyse HeLa cells was omitted. Therefore, the pelleted infected HeLa cells were lysed in 1 ml of deionized distilled water ($ddH_2O$) by passing the suspension 10 times through a 27-gauge needle before high-speed centrifugation in Percoll. The band distribution after centrifugation included only a top band of cell debris and two bottom bands. The upper bottom band (1.061 to 1.074 g/ml) contained cell debris and bacteria; the lower bottom band (>1.074 g/ml) contained the intracellular bacteria. Bacteria from the lower bottom band were routinely washed twice in phosphate-buffered saline or $ddH_2O$ to remove residual Percoll.

**Microscopy.** Electron microscopy (EM) was performed with standard protocols in the EM facility of the Faculty of Medicine, Dalhousie University. Briefly, specimens prepared for thin sectioning were fixed with 2.5% (vol/vol) glutaraldehyde in 0.1 M cacodylate buffer, pH 7.2, for 2 h, rinsed with three 10-min changes of cacodylate buffer, and postfixed with 1% (wt/vol) $OsO_4$ in cacodylate buffer for 2 h. Alternatively, in an attempt to improve the preservation of the bacterial cell envelope, we used the Karnovsky fixation protocol (41), which is based on a combination of freshly depolymerized paraformaldehyde and glutaraldehyde as the primary fixative.

For this protocol, 2 g of paraformaldehyde was slowly dissolved in 15 ml of $ddH_2O$ by heating to 60°C and stirring. One to three drops of 1 N NaOH were added with stirring to completely clear the solution as it cooled to room temperature. Then, 10 ml of 25% (vol/vol) glutaraldehyde was added, and the volume was brought to 50 ml with 0.2 M cacodylate buffer, pH 7.4 to 7.6. A modification of the original protocol was not to add $CaCl_2$. Samples were fixed in Karnovsky fixative for 2 h at room temperature, followed by three 10-min washes in cacodylate buffer and postfixation in osmium tetroxide as indicated above. The osmium tetroxide was washed from all specimens with three 10-min cacodylate buffer changes. All samples were prestained overnight in blocs with 0.25% (wt/vol) aqueous uranyl acetate, dehydrated in a graded series of acetone up to 100%, and embedded in epoxy (TAAB 812/Araldite) resin. Ultrathin sections of a gold-silver shade (≈80 nm thick) were cut in an LKB Ultracut microtome with a diamond knife. Ultrathin sections were then poststained for 10 min with 2% (wt/vol) aqueous uranyl acetate, followed by freshly prepared modified Sato's lead citrate (34) for 4 min. For the latter, 10 to 30 mg of lead citrate was dissolved in 10 ml of freshly boiled $ddH_2O$ previously cooled to room temperature and made alkaline with 3 drops of 10 N NaOH. This lead citrate solution was filtered through a Nalgene syringe filter (0.2-μm pores) before use.

For freeze fracturing, bacteria were either suspended in $ddH_2O$ and quick frozen or treated for 30 min with 20% glycerol or a combination of 20% glycerol and 2% glutaraldehyde in $ddH_20$ before freezing. To achieve quick freezing, a 2- to 3-μl drop of a thick suspension of bacteria ($10^{10}$ to $10^{11}$/ml) was placed on gold stubs and immersed in either liquid Freon 22 or liquid propane held in the top cavity of a stainless steel rod immersed in liquid nitrogen. Frozen samples were fractured at −105°C in a Balzers-360 freeze fracture unit (Balzers Instruments, Balzers, Liechtenstein), in situ shadowed with platinum-carbon (with a Balzers EVM 052 control unit), and then covered with a thin film of carbon from a carbon arc resistance gun. The gold stubs were taken from the Balzers-360 unit and brought to room temperature to melt the replicated specimen. The replicas were then floated on the surface of clean $ddH_2O$ and transferred to a 5.25% (vol/vol) solution of sodium hypochlorite (by means of a platinum loop) for not less than 6 h to eliminate residues of organic material. Replicas were floated in a series of $ddH_2O$ drops (to rinse the hypochlorite) and picked up on 200-mesh, formvar- and carbon-coated grids for observation.

All EM samples were observed in a Philips EM300 transmission electron microscope operating at 60 kV. Micrographs were taken with a 35-mm camera with Kodak FGP film. All materials and reagents for EM were obtained from Marivac Ltd. (Montreal, Canada) and were of biological grade.

**Image analysis.** Photographic negatives of representative forms showing unique features were printed to the same magnification (100,000×) on Ilford Multigrade IV RC Deluxe photographic paper (Ilford Imaging Canada Ltd., Markham, Canada). High-definition areas from these prints were scanned in an Epson ES-1200C scanner (Seiko Epson Co., Nagano, Japan) at a resolution of 1,200 pixels per inch (ca. 470 pixels per cm). The scanned images were then analyzed, after the concept originally developed by Graham and Beveridge (31), with the line profile function of the ImagePro 4.0 software (Media Cybernetics Inc., Silver Spring, Md.). In high-definition areas where the bacterial cell envelope was straight (usually along the sides of longitudinal sections), we performed perpendicular scans of the envelope with the thick-line option, which yields average intensity readings of all the pixels found between two preset parallel lines for each distance increment. High-definition areas at the bacterial cell poles (where the envelope curves) were typically analyzed with the normal-line option, which yields single-pixel intensity values along a preset line for each distance increment.

In contrast to the densitometry values reported by Graham and Beveridge (31), our digital analysis generated intensity data of the envelope profiles, where a value of 255 represents pure white (that is, a completely electron-transparent material) and a value of 0 represents pure black (that is, maximum electron opacity). Intensity traces across the bacterial cell envelope were produced by exporting profile data from ImagePro 4.0 into SigmaPlot 5.0 (SPSS Inc., Chicago, Ill.) and graphing the intensity readings against distance increments (in nanometers) across the trace. Our graphs therefore appear inverted in relation to those based on densitometry measurements and should be interpreted accordingly.

## RESULTS

***L. pneumophila* growth phases in HeLa cells.** Using previously reported morphological and physiological responses of HeLa cells to *L. pneumophila* infection (17, 29, 30), we divided the intracellular growth cycle shown in Fig. 1 into four phases, centered on the well-defined event of bacterial replication. In addition, Fig. 1 incorporates intracellular events reported for other mammalian cells and protozoa (1, 16, 39, 51), as well as known bacterial responses (referenced in the legend), to allow a comprehensive application.

The binding of *L. pneumophila* to surface receptors and its subsequent uptake into phagosomes (Fig. 1, step 1), together with the association of the *L. pneumophila*-containing phagosomes with vesicles and mitochondria (Fig. 1, step 2), defined

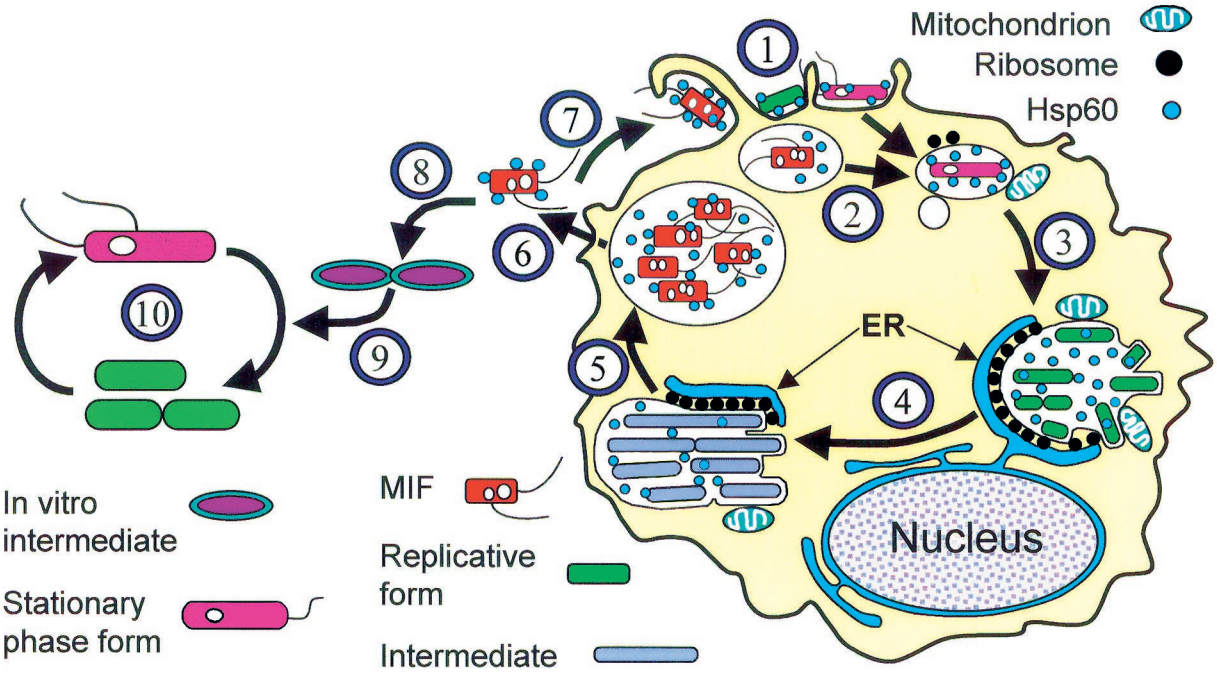


FIG. 1. Schematic representation of intracellular and extracellular growth cycles of *L. pneumophila*. 1, Different *L. pneumophila* forms may attach to and enter a host cell (protozoan, macrophage, or cell line). Surface-exposed Hsp60, at least in part, mediates attachment and cell entry (28). Mature intracellular forms (MIFs) are often internalized by macrophages through coiling phagocytosis (15, 16). 2, After entry, MIFs and stationary-phase bacteria grown in vitro downregulate flagellar genes (13), inhibit phagosome-lysosome fusion (40), and recruit vesicles and mitochondria around the phagosome (20, 29, 39, 51). Exponential-phase replicative bacteria cannot effectively proceed through this step (40). Synthesis of Hsp60 is upregulated, and this protein is released into the phagosomal space (19). Expression of the Dot/Icm proteins (6, 11, 56, 59) and other factors (40) is required to abolish phagosome-lysosome function and further conditioning of the phagosome. 3, The phagosome associates with the endoplasmic reticulum (ER) (1, 63, 64) to form the replicative compartment. Active replication takes place in ribosome-studded vacuoles. While we have depicted the endoplasmic reticulum and the legionella-containing vacuole as separate entities that remain associated, it has recently been suggested that they form a single continuous compartment (64). The pattern of *L. pneumophila* protein expression changes (2, 62), and Hsp60 accumulates in the vacuolar space (25). 4, Intermediate forms with a distinct morphology and tinctorial properties arise (27), while replication continues. 5, Termination of intracellular replication leads to full differentiation of MIFs, which acquire a full-virulence phenotype (16, 27, 55) as well as a bright red color after the Gimenez stain and numerous inclusions (16, 26, 27, 29). Flagellum expression and cytotoxicity are upregulated (13), and the abilities to lyse the vacuolar membrane (5) and assemble DotO/H proteins on the bacterial cell surface (65) are induced. 6, MIFs are released to the extracellular medium, either free or inside vesicles. The released bacteria may carry bound host proteins (7) and display unique ultrastructural, physiological, and surface properties (7, 15, 16, 27). 7, MIFs or MIF-packed vesicles (9, 12, 55) may initiate another intracellular cycle. 8, Released MIFs may also start an extracellular growth cycle. Because MIFs do not replicate, differentiation into a replicative intermediate is required (26). 9, Intermediates eventually differentiate into the exponential-phase, actively replicating form (26). 10, In the extracellular growth cycle, *L. pneumophila* alternates between exponential-phase forms and stationary-phase forms (13). Entry into stationary phase is linked to enhanced virulence and improved resistance to environmental challenges, likely through a complex regulatory network (13, 33). The changing colors of bacteria reflect their tinctorial properties after the Giménez stain. Red is regarded as a Giménez-positive stain, green as a Giménez-negative stain, and purple as a Giménez-intermediate stain (27).

the prereplicative phase. The early replicative phase was defined by a clear association of *L. pneumophila*-containing vacuoles with ribosomes and what appeared to be the endoplasmic reticulum (Fig. 1, step 3). Vacuoles could contain one or several bacteria (not necessarily undergoing cell division), and the vacuolar membrane would closely follow the contour of enclosed bacteria. The late replicative phase was defined by the formation of complex vacuoles with a multilobular structure (perhaps formed by the endoplasmic reticulum) containing numerous bacteria clearly undergoing cell division (Fig. 1, step 4). The vacuolar membrane became considerably expanded but continued to be associated with both ribosomes and mitochondria and often tightly followed the contour of the enclosed bacteria. Finally, the postreplicative phase was characterized by the presence of nonreplicating bacteria loosely contained in a vacuole exhibiting a more spherical outline and not associated with cell organelles (Fig. 1, step 5). Free legionella-laden vesicles were commonly seen floating in the culture supernatant at this stage.

We used these well-defined host cell responses as timing landmarks for the *L. pneumophila* intracellular cycle; therefore, our emphasis remained focused on bacterial morphology. Except for those specimens processed by freeze fracture, the morphological observations presented below contain strictly two-dimensional information, as seen in ultrathin sections.

***L. pneumophila* morphology in the prereplicative phase.** Because we initiated infection with two different types of inoculum, we describe each separately.

**(i) Infection with plate-grown *L. pneumophila*.** The plate-grown rods used in the inoculation exhibited a diameter that varied from 0.3 to 0.5 μm and a length of between 1.5 and 3.0 μm (Fig. 2A). The cytoplasmic region was rich in ribosomes

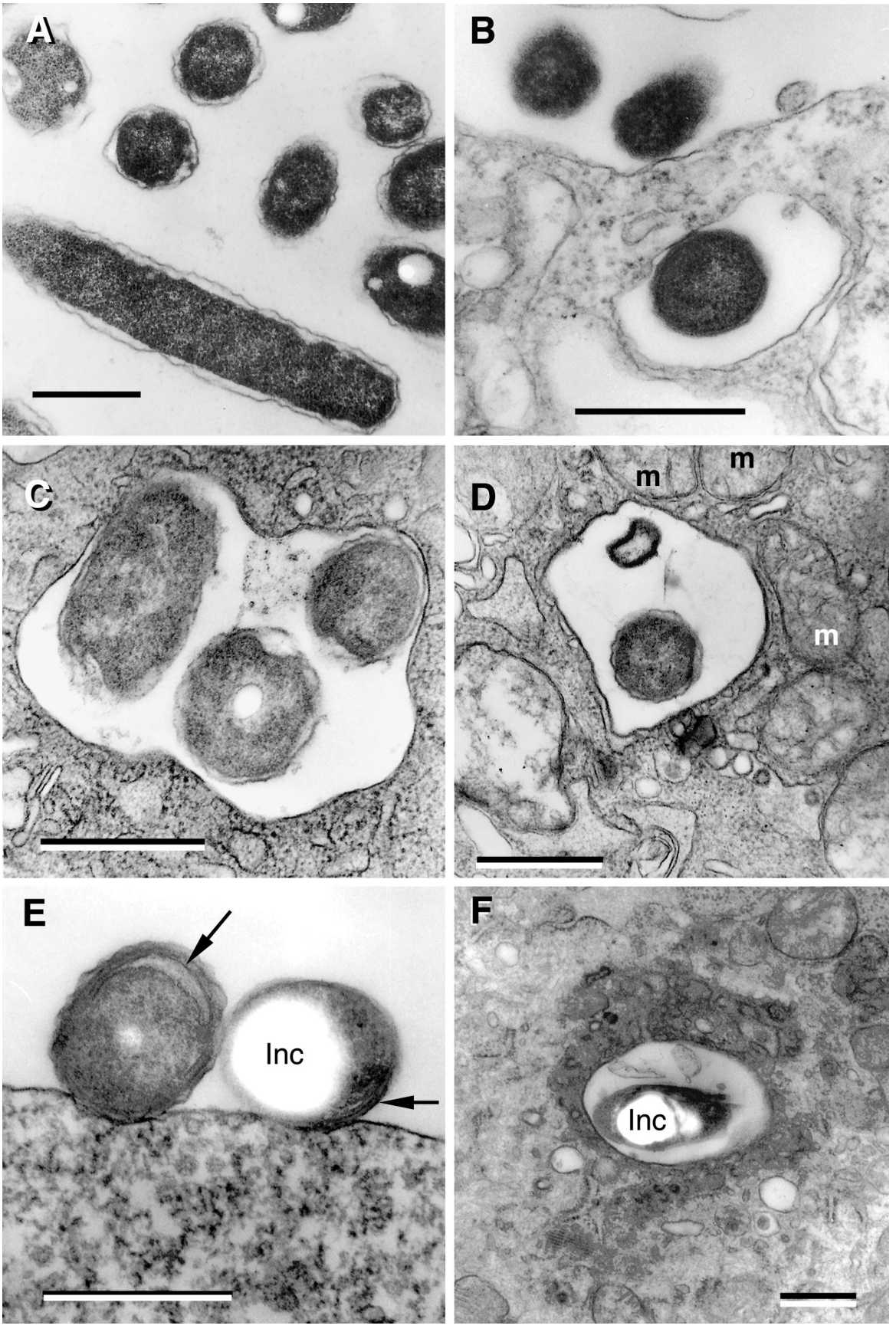
A
B
C
D
m
m
m
E
Inc
F
Inc

and uniform in electron density. Besides the nucleoid and small inclusions, sectioned bacteria depicted no other significant substructure. Rods displayed a typical gram-negative envelope consisting of clearly defined outer and inner membranes of equal width (≈7.5 nm). The outer membrane appeared wavy, and the periplasmic region between the outer and cytoplasmic membranes was electron lucent, with no discernible peptidoglycan layer. At 6 h postinfection, the inoculated rods were found bound to the HeLa cell surface or in vacuoles, either singly or in small groups of two to three (Fig. 2B and C), with no changed morphology. Surface-bound bacteria and bacteria contained singly in peripheral phagosomes were also seen in specimens fixed at 12 h postinfection. At this time, the vacuoles containing bacteria, initially found in the periphery of HeLa cells, took a more central cytoplasmic position as they became associated with mitochondria (Fig. 2D).

**(ii) Infection with *L. pneumophila* grown in HeLa cells.** The unique general morphology of host cell-grown *L. pneumophila* has been described previously (16, 27, 29) and will be further described in great detail in a later section. At 3 to 6 h postinfection, HeLa cell-grown bacteria were seen bound to the surface of HeLa cells (much more often than plate-grown legionellae) (Fig. 2E) or singly internalized in vacuoles frequently surrounded by a cloud of vesicles and mitochondria (Fig. 2F). There was no change in bacterial morphology (in relation to the inoculum) during the prereplicative phase.

***L. pneumophila* morphology in the early replicative phase.** The first stages of this phase (observed as early as 6 h postinfection) were marked by an expansion of the legionella-containing vacuole, which created a space much greater than necessary to house the enclosed SVir or 2064 bacteria (Fig. 3A and B). However, at later times (≈12 h postinfection), SVir legionellae were found surrounded more tightly by the vacuolar membrane (Fig. 3C and D). This apparent contraction of the once expanded vacuolar membrane was only seen in less than 5% of the vacuoles containing legionellae of the 2064 strain. The key event of this phase, however, was the decoration of the cytoplasmic side of the vacuolar membrane with ribosomes and/or its apparent association-fusion with the rough endoplasmic reticulum (64), marked with arrowheads in most of the panels of Fig. 3. In relation to the 6-h specimens (containing up to three bacteria per phagosome), the number of bacteria per vacuole at 12 h postinfection had increased by 10-fold (Fig. 3E). This sharp increase in bacterial numbers per vacuole clearly entailed bacterial multiplication. Up to this time, no major changes in bacterial morphology occurred in relation to the original plate-grown inoculum; a minor change perhaps including a more tapered appearance of the bacterial poles.

Importantly, in specimens inoculated with HeLa-grown *L. pneumophila*, the bacteria contained in early-replicative-phase vacuoles decorated with ribosomes now displayed a standard gram-negative envelope ultrastructure and a uniform cytoplasm rich in ribosomes with no significant substructure (Fig. 3F). This clearly implied that the unusual morphology of HeLa-grown *L. pneumophila* (see below) had dramatically reverted to that typical of plate-grown or replicative legionellae. Unfortunately, we were unable to definitely identify any morphological intermediates in vacuoles of HeLa cells infected with HeLa-grown legionellae even after a thorough observation of numerous ultrathin sections. In all cases, cell division occurred through a pinching, nonseptated process, as shown in Fig. 3D.

***L. pneumophila* morphology in the late replicative phase.** Contrasting morphological changes were evident in replicating bacteria contained in multilobular large vacuoles. The majority of sectioned bacteria at this phase (≈70%) developed a very apparent waviness (sharp ripples) in their outer membrane (Fig. 4A). Another 13% developed a rather straight outer membrane and a difficult-to-resolve inner membrane. The membranes, periplasm, and cytoplasm acquired a remarkably homogeneous electron density throughout (Fig. 4B). For the 2064 strain, outer membranes with sharp ripples could be seen as early as 12 h postinfection (Fig. 4C), but they were also apparent in the late replicative phase (12 to 25 h) (Fig. 4D, arrows). Finally, about 4% of the sectioned bacteria clearly showed invaginations of the inner membrane (Fig. 4E, arrowheads).

In this late replicative phase, cytoplasmic inclusions became evident in all the described morphological forms, but clearly were more abundant in those bacteria depicting an outer membrane with ripples or a straight envelope (of which 32% and 50%, respectively, had inclusions). The number of bacteria per replicative vacuole reached its maximum (up to 100 bacteria per sectioned vacuole) during this phase (Fig. 4F). As depicted in Fig. 4F, different morphological types could be found within the same vacuole, implying that at this time, the differentiation process either was not synchronous or was independently controlled in each vacuole.

***L. pneumophila* morphology in the postreplicative phase.** In the final stages of HeLa cell infection (recognized by the presence of enlarged spherical vacuoles loosely containing bacteria no longer undergoing cell division), *L. pneumophila* experienced dramatic changes in morphology (Fig. 5). Postreplicative-phase bacteria (previously referred to as mature intracellular forms [MIFs]) (26, 27, 38) were seen as short rods with blunt ends and a very pleomorphic envelope. It should be recognized that the term MIF is used here to represent a distinct morphological group and not a single form. Therefore, MIFs include forms with the following dominant features: (i) long inner membrane invaginations (i.e., multilayered envelope) (Fig. 5A), (ii) a thickening of the inner leaflet of the

FIG. 2. *L. pneumophila* morphology in the prereplicative phase. (A) Plate-grown legionellae (strain 2064 shown) with a standard gram-negative morphology, used as the inoculum to infect HeLa cells. (B) The overall bacterial morphology did not change during binding or internalization (strain SVir at 6 h postinfection shown). (C) More than one morphologically unchanged bacterium (SVir shown) could colocalize in early vacuoles. (D) Morphologically unchanged bacterium (SVir shown) in a vacuole surrounded by mitochondria (m) and vesicles. (E) HeLa-grown legionellae (SVir shown) tightly bound to the surface of a HeLa cell. Note the unique envelope morphology (multimembranous envelope) (arrows) of the bound bacteria and the prominent inclusion (Inc) in one of them. (F) HeLa-grown legionellae (2064 shown) inside an early vacuole surrounded by a multitude of vesicles. Note the bubble in the bacterial cytoplasmic region produced by a poorly embedded inclusion. Bars, 0.5 μm.

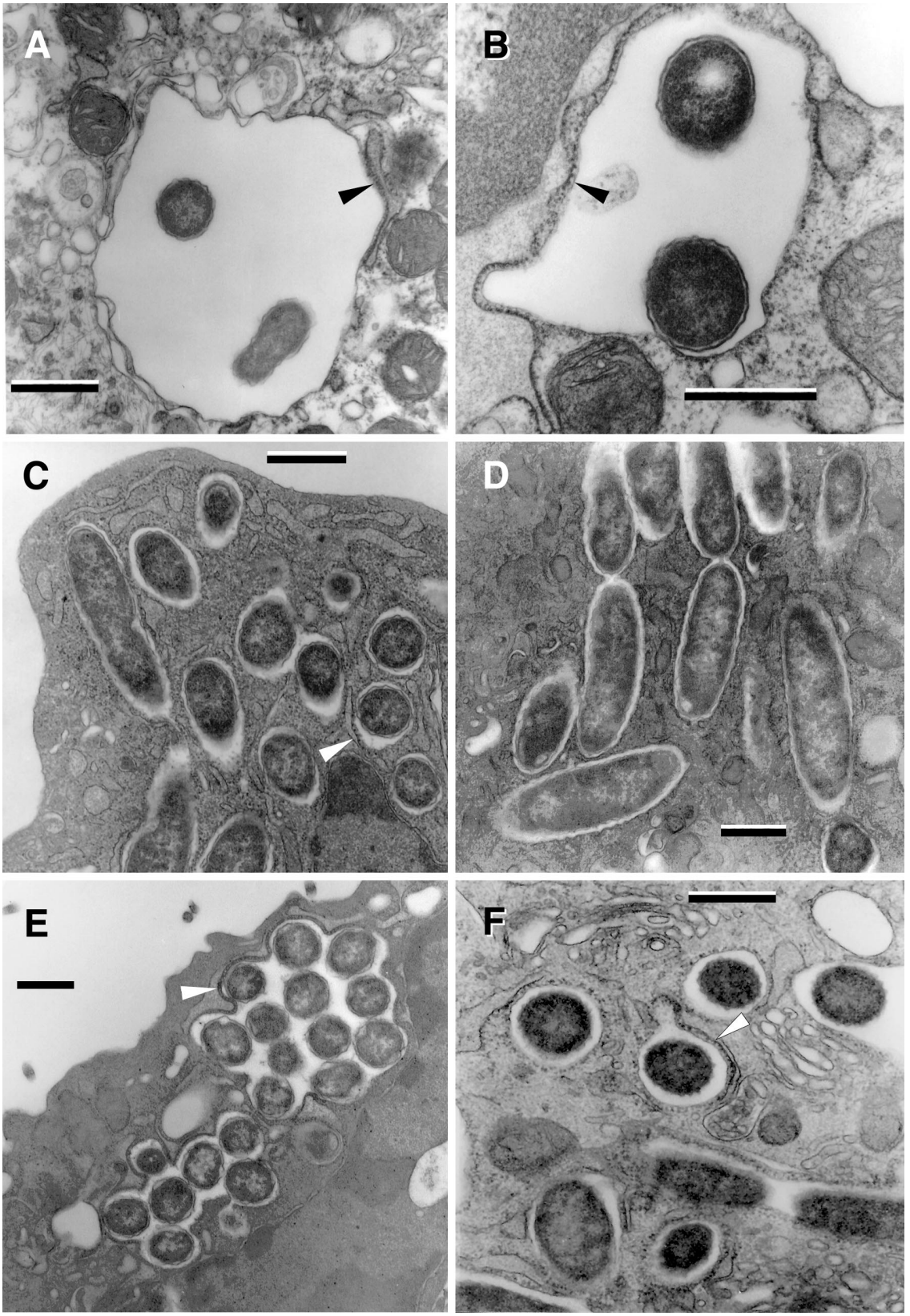


FIG. 3. *L. pneumophila* morphology in the early replicative phase. Loose enlarged vacuoles associated with rough endoplasmic reticulum (arrowheads) and containing morphologically unchanged 2064 (A) or SVir (B) bacteria from a plate-grown inoculum, at about 6 h postinfection. (C) At 12 h postinfection, morphologically unchanged SVir bacterial cells from a plate-grown inoculum were often seen individually contained in tight vacuoles. (D) Morphologically unchanged and replicating SVir bacteria from a plate-grown inoculum in tight vacuoles that followed the contour of the enclosed bacteria. (E) Many vacuoles prominently surrounded by ribosomes and/or rough endoplasmic reticulum contained numerous bacteria (SVir shown at 12 h postinfection). Note the vacuolar membrane closely following the contour of the contained bacteria. (F) Bacteria from a HeLa cell-grown inoculum singly contained in tight vacuoles and showing the replicative morphology (strain 2064 at about 20 h postinfection). Bars, 0.5 μm.

outer membrane (i.e., banded envelope) (Fig. 5B), and (iii) an irregular shape and dense cytoplasm (Fig. 5C and D).

A typical in vacuole bacterial population consisted of cells exhibiting one of these dominant features alone or combinations of two or three features in the following proportions: banded alone, 21.4%; banded with an irregular shape, 23.4%; banded and multilayered, 6.5%; banded with an irregular shape and multilayered, 11.0%; multilayered alone, 18.8%; and multilayered with an irregular shape, 18.8%. More than 70% of MIFs contained inclusions (1 to 5 per sectioned bacterium). Although sometimes the long invaginations of the inner membrane ran along the cytoplasmic inclusions, our observations did not agree with those of Keel et al. (43), who reported that intracellular inclusions are membrane bound.

**Putative morphological intermediates of the replicative-to-mature-form transition.** In an attempt to increase the likelihood of identifying short-lived morphological intermediates, we purified the infecting bacteria from several 75-$cm^2$ HeLa monolayers in self-generated, continuous-density gradients. Bacteria were harvested in mid- to late exponential phase, previously determined to occur at ≈36 h postinfection (27). This allowed the examination of much larger numbers of bacteria than found inside the vacuoles of infected cells, providing the opportunity to evaluate a broader range of legionellar forms.

Besides replicating bacteria with a typical gram-negative envelope, which comprised up to 45% of the purified bacteria, we found two other morphologically distinct forms. In agreement with our in vacuole observations (Fig. 4A to D), the most abundant of these two forms (≈40% of the purified bacteria) showed a very wavy outer membrane (Fig. 6A) and was considered to be equivalent to the form with sharp ripples shown in Fig. 4A and C. Interestingly, the outer membrane ripples of the purified forms had a longer wavelength than those of the intravacuolar forms. A morphological feature clearly present in the purified forms but not observed in the intravacuolar forms with wavy outer membranes was what we interpreted as cytoplasmic fragmentation (Fig. 6B), which in some cases was rather extreme (Fig. 6C).

The other form (≈15% of the purified bacteria) depicted a high degree of envelope smoothness (very straight outer membranes). Because the electron density was quite uniform throughout these forms, the inner membrane was difficult to discern (as in the form marked with an arrow in Fig. 6D). These intermediate forms with straight outer membranes could depict either small or no inclusions (Fig. 6D) or prominent inclusions (Fig. 6E). In vacuole equivalents to these forms were identified (e.g., Fig. 4B). A variant of these forms with straight outer membranes (only seen in less than 5% of the purified bacteria) displayed stretches of well-defined membranes and an incipient thick layer (Fig. 6F). In vacuole equivalents of these forms were also found (not shown).

**Morphological intermediates of the mature-to-replicative-form transition in vitro.** It was mentioned above (*L. pneumophila* morphology in the early replicative phase) that we were unable to definitely identify in vacuole morphological intermediates of the MIF-to-replicative-form transition. Therefore, we grew purified MIFs in vitro (previously reported to yield morphological intermediates [26]) to carry out a detailed ultrastructural analysis of observable changes. Purified MIFs were incubated in BYE broth at 37°C, and samples were taken at different times for ultrastructural observations and to perform viable-cell counts. We confirmed previous observations of "intermediate" forms beginning to show up at the end of a long lag phase and the onset of bacterial replication. A striking feature of these intermediates was the presence of a loose wavy outer membrane and a well-defined periplasm containing vesicles (marked with arrows in Fig. 7A and B). A number of sections again depicted a standard gram-negative ultrastructure typical of replicative legionellae, i.e., no prominent inclusions, a well-defined outer membrane, and a ribosome-rich cytoplasm (Fig. 7B).

Within the exponential phase of growth in BYE broth, the forms with a standard replicative morphology reached almost 100% (Fig. 7C), but during stationary phase, up to 30% of the sectioned bacteria displayed internal membranes (sometimes very difficult to distinguish) stacked similarly to those in the postreplicative-phase MIFs (Fig. 7D). We did not observe stationary-phase forms with a thick layer or irregular dark laminated envelopes, confirming that they never fully acquired all the complex characteristics of MIFs, as reported previously (27).

***L. pneumophila* envelope profiles.** Envelope profiles were best depicted as plots of pixel intensity (i.e., an inverse correlate of electron density) versus distance across the envelope. Plots constituted an unbiased way to characterize the physical-morphological properties of the membranes and layers that formed the envelope of the many different forms described, as well as the size and electron density of the periplasm. We could classify all the profiles analyzed into five major groups showing very distinctive features (Fig. 8).

Group 1 included what we called the standard gram-negative envelope, clearly displaying an inner membrane, an electron-lucent periplasmic space, and a wavy outer membrane. The two leaflets of the inner and outer membranes had a similar spacing and intensity (Fig. 8A). All replicative forms displayed this profile in vitro and in vivo, as did the majority (70 to 80%) of stationary-phase forms in vitro. When HeLa cells were infected with bacteria grown in vitro, this envelope morphology prevailed until the late replicative phase, when intermediate forms with different envelope profiles began to appear.

Group 2 included all profiles with a defined inner and outer membrane, generally very straight (smooth), and a thick, electron-dense layer associated with the inner leaflet of the outer membrane (Fig. 8B). Image analysis clearly indicated that this thick layer constituted a distinct structure, as indicated by the wide dark peak overlapping that corresponding to the inner leaflet of the outer membrane (IL-OM in Fig. 8B), which appeared at the conserved distance of ≈5 nm from the outer leaflet of the outer membrane. In all cases, an electron-translucent region between the dense band and the inner membrane (corresponding to the periplasmic space) was still evident (Fig. 8B). It should be noted that a consistent characteristic of the profiles within this group was the difference in intensity between the two leaflets of the inner and outer membrane, reflected as peaks of different depth (Fig. 8B). Group 2 profiles were restricted to late-replicative-phase forms (e.g., Fig. 6F) and to postreplicative-phase forms.

Profiles showing more than two membrane bilayers were placed in group 3. Although the most common number of

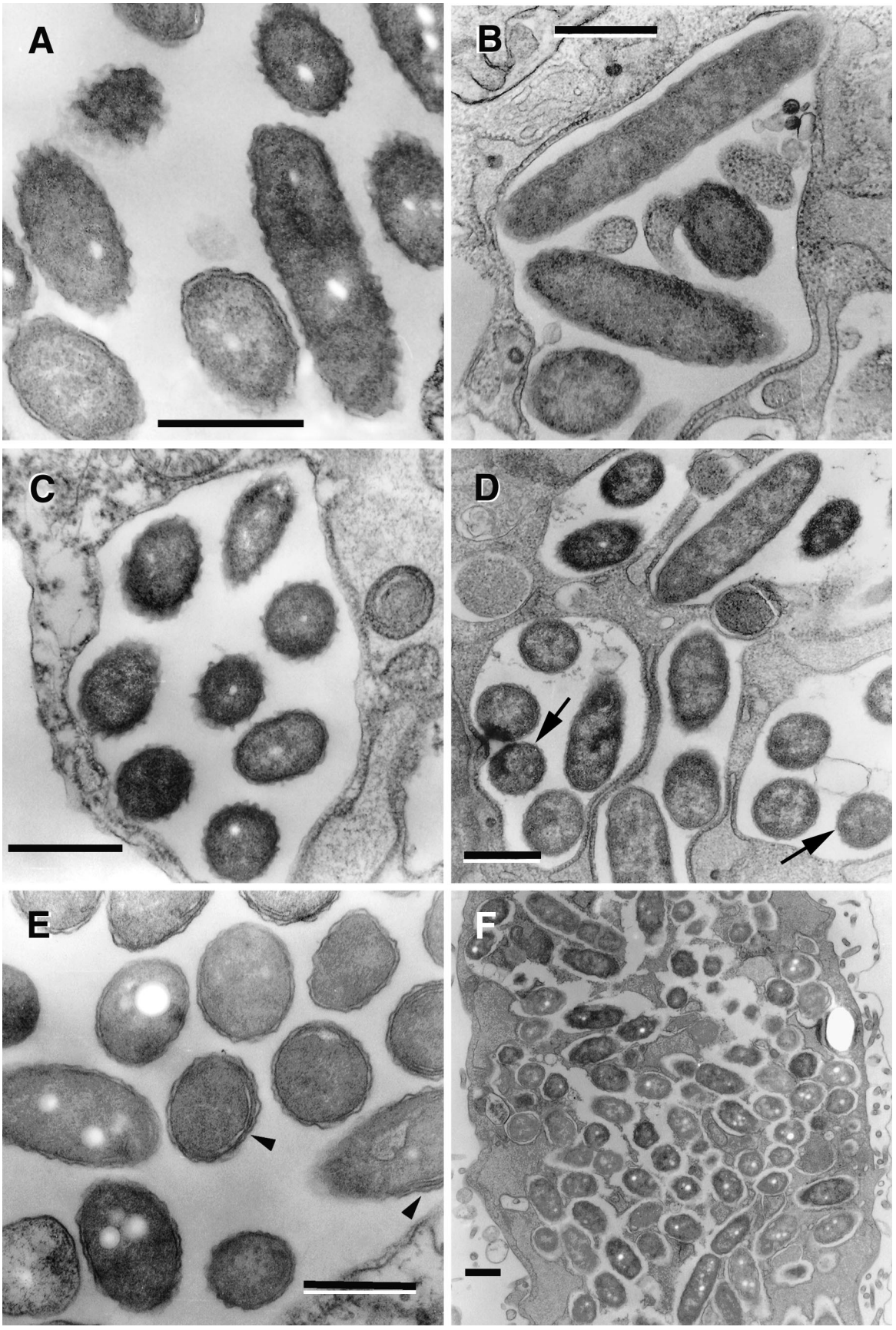
A
B
C
D
E
F

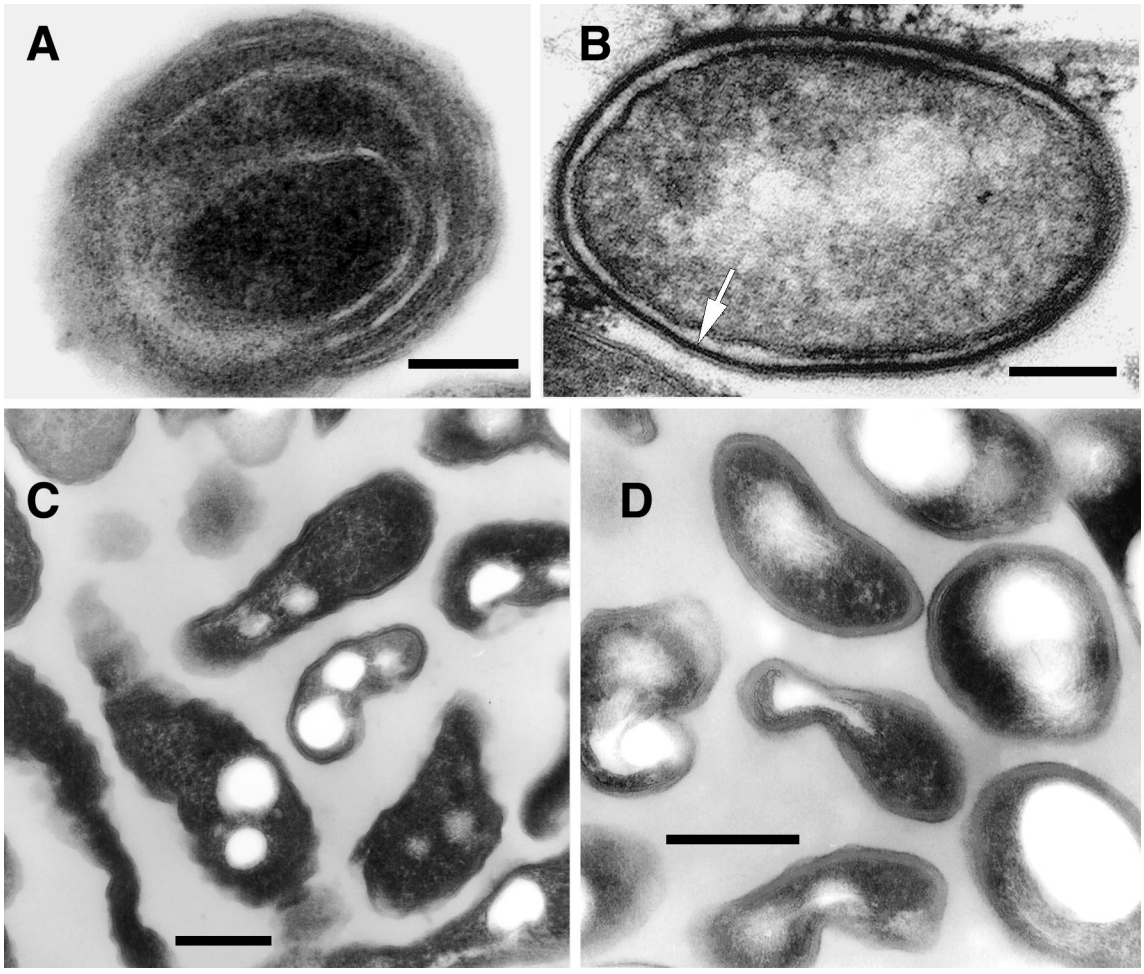


FIG. 5. *L. pneumophila* morphology in the postreplicative phase. (A) Extended invaginations of the inner membrane that resulted in a multilayered envelope (SVir strain shown at 48 h postinfection). Bar, 0.25 μm. (B) Section of SVir (bacterium found free in the supernatant of infected HeLa cells 3 days postinfection) showing the characteristic thick layer associated with the inner leaflet of the outer membrane (arrow). Postreplicative SVir forms typically had irregular shapes, as shown in specimens fixed with our standard protocol (C) (bar, 0.1 μm) or the Karnovsky fixation protocol (D) (bar, 0.25 μm). Note that the Karnovsky protocol yielded slightly smoother envelopes.

stacked bilayers was four (including the outer membrane), as shown in Fig. 8C, envelopes with as many as six bilayers in total were not unusual (Fig. 8D). Examples of three stacked bilayers (Fig. 8E) were rare, as this configuration implies that the large central compartment (marked with a p) corresponds to an enlarged periplasmic space. The outer membrane in the profiles of group 3 could be associated (or not) with a thick electron-dense layer. The profile depicted in Fig. 8C strongly suggested that the internal membranes were invaginations of the inner membrane. On the one hand, the relative intensities of the two leaflets (peak's height) were a mirror image of the immediate-neighbor membrane. On the other hand, the material present between internal membranes alternated between light and dark. The electron-dense dark material, usually laid between the inner membrane and first internal membrane (and between the fourth and fifth membranes in Fig. 8D) most likely corresponded to the cytoplasm, whereas the electron-light material between the first and second internal membranes (or between the fifth and sixth internal membranes in Fig. 8D) most likely corresponded to the periplasm. Multimembranous envelopes did not always show a marked density differential between leaflets and were typically present in postreplicative-

FIG. 4. *L. pneumophila* morphology in late replicative phase. (A) SVir bacteria displaying an electron-dense cytoplasm and an outer membrane with sharp ripples, 25 h postinfection. Note that these morphologically distinct bacteria coexisted with bacteria displaying a standard gram-negative envelope and a less electron-dense cytoplasm. (B) Some bacteria (strain 2064 from a HeLa cell-grown inoculum is shown at 21 h postinfection) developed a rather straight (smooth) outer membrane. The envelope in these bacteria was often difficult to resolve. (C) In the 2064 strain, forms with sharp ripples could be seen at 12 h postinfection but also persisted until later times (D) (arrows), when they coexisted with the smooth-outer-membrane intermediates. (E) Late-replicating bacteria (SVir shown at 25 h postinfection) showed invaginations of the inner membrane (arrowheads). (F) Intricate replicative vacuole containing numerous SVir bacteria with some of the distinctive morphologies described for panels A to E is shown. Bars, 0.5 μm.

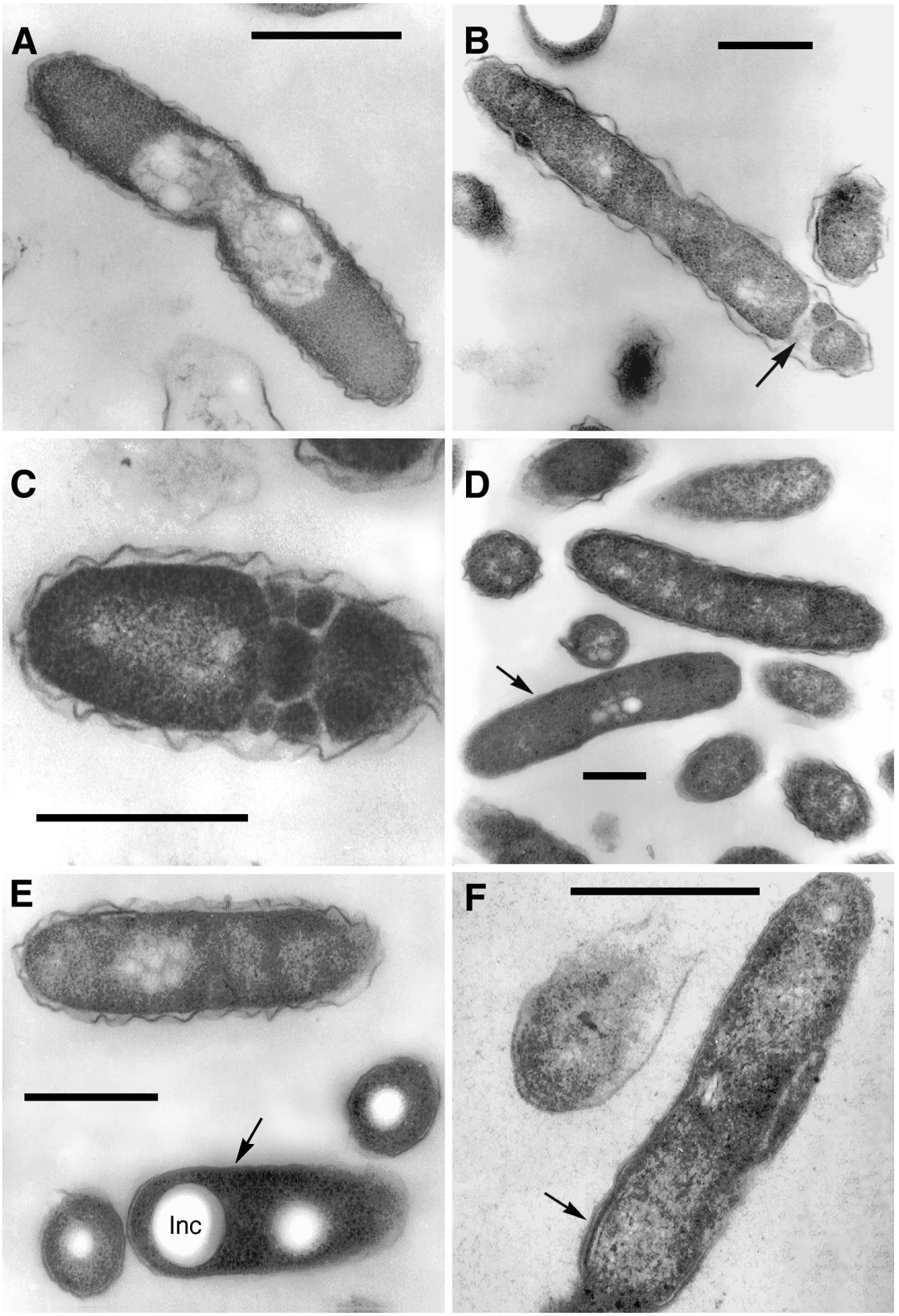


FIG. 6. Morphological forms present in purified populations of replicating intracellular legionellae. (A) Intermediate SVir replicative form with sharp ripples in the outer membrane. (B) SVir intermediate with wavy outer membrane and fragmented cytoplasm at one of the poles (arrow). (C) SVir bacterium depicting pronounced fragmentation. The form shown appears to have been fragmented, possibly due to excessive membrane invagination. (D) Intermediate strain 2064 form (arrow) with a very homogeneous appearance and very straight membranes. Note the morphological differences between this form and the neighbor form above it, which has a typical gram-negative envelope ultrastructure. (E) An intermediate SVir form (arrow) with a very straight outer membrane, a difficult-to-resolve inner membrane, and prominent well-defined inclusions (Inc). (F) Replicative 2064 intermediate similar to that shown in panel D but displaying an incipient thick layer (arrow). Bars, 0.5 μm.

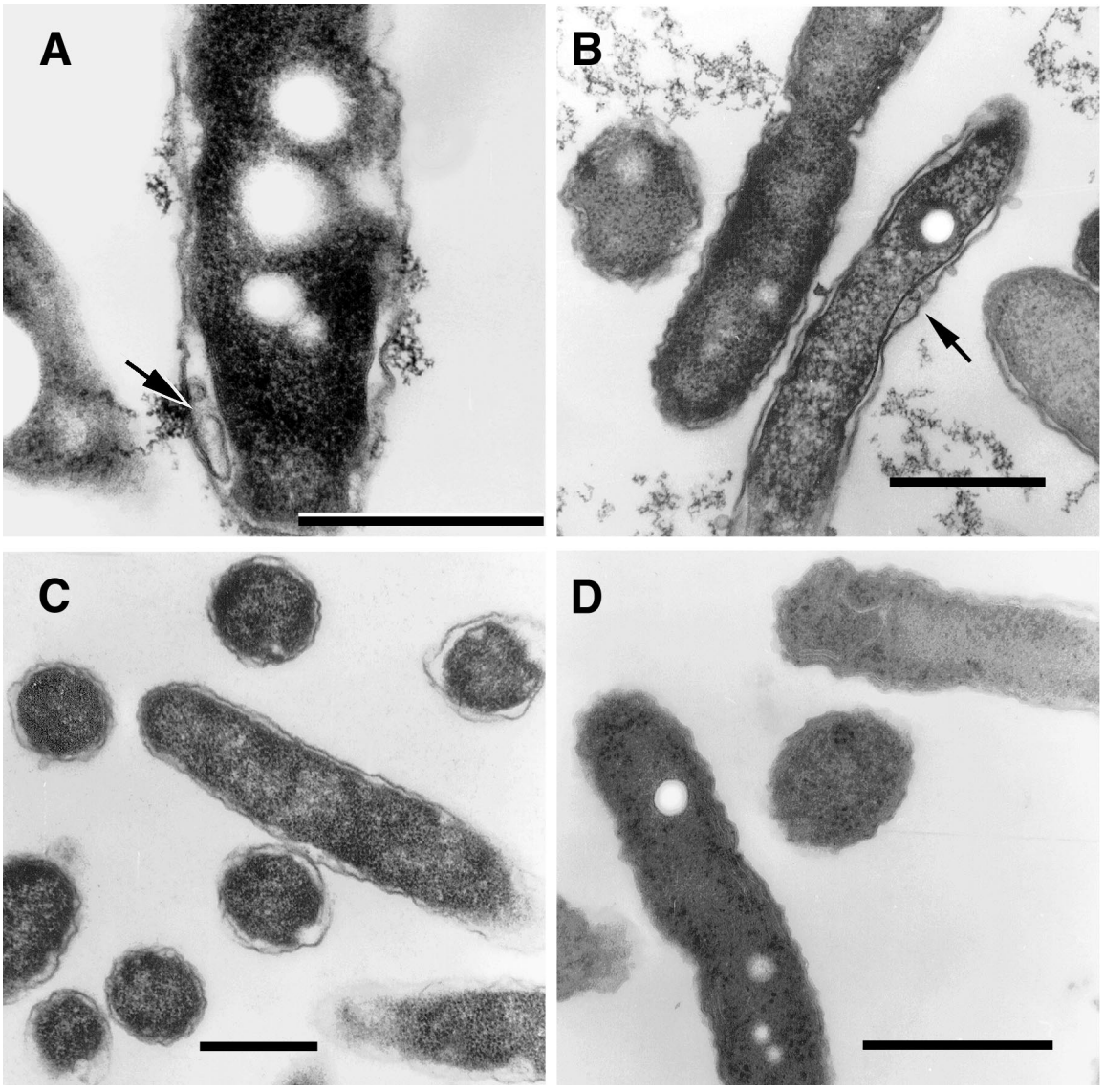


FIG. 7. In vitro intermediates of the MIF-to-replicative-form transition. (A) Strain 2064 intermediate depicting intraperiplasmic vesicles (arrow). (B) An SVir intermediate with several intraperiplasmic vesicles (arrow) is shown side by side with a section of a replicating bacterium depicting a standard gram-negative ultrastructure. (C) Typical replicative 2064 forms derived from MIFs ≈20 h after inoculation into BYE broth. (D) Stationary-phase 2064 intermediate with multiple internal membranes but a generally unresolved envelope. Bars, 0.5 μm.

phase forms as well as in a small proportion of stationary-phase forms in vitro. Interestingly, the multimembranous envelopes of stationary-phase forms had no evidence of a distinct outer membrane and periplasm, as all structures had a very similar intensity (e.g., Fig. 7D).

Group 4 comprised all profiles with no well-resolved inner membrane. At first, we were hesitant to include these profiles as a group because their distinctive characteristic could be the result of a processing artifact. However, we encountered numerous examples of envelopes with a visually unresolved inner membrane side by side with impeccably preserved envelopes, suggesting that this characteristic was not the result of a general fixation deficiency. On the other hand, the outer membrane was, in most cases, quite well preserved (e.g., Fig. 8F). Envelopes of group 4 were typically associated with intermediates found exclusively in late replicative phase (e.g., Fig. 4B and D).

In group 5, an electron-dense thick layer (introduced as the distinctive characteristic of group 2) was apparently embedded in a very dense periplasm, in turn bordered by membranes that were also dense. The overall appearance of these envelopes was that of a spore-like laminated coat (Fig. 8G). In extreme cases, a defining outer membrane or other substructural details were barely visible, and the thick envelope appeared as a single dark layer with a striking similarity to a gram-positive cell wall. Group 5 profiles were restricted to postreplicative-phase MIFs.

**Freeze-fractured specimens.** *L. pneumophila* MIFs and in vitro-grown legionellae (cultured in BYE broth or BCYE agar plates) showed a number of important morphological differences when studied by freeze fracture. Although some agar-

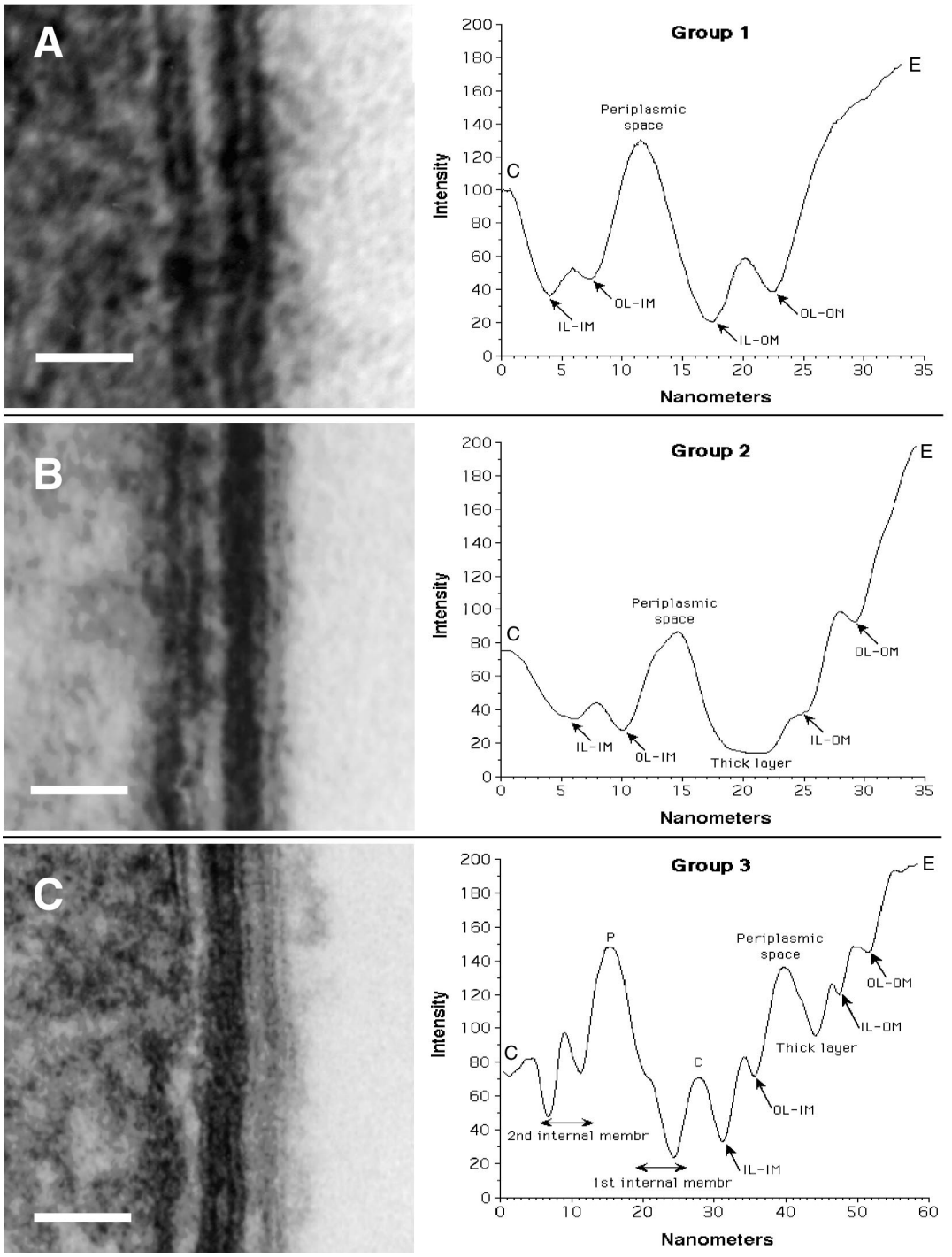


FIG. 8. Envelope profiles comprising different groups of legionellar forms. Electron micrographs shown on the left side were used to obtain the envelope profiles shown to the right of each panel. (A) Group 1 pattern consisted of the typical gram-negative envelope with inner and outer membranes separated by a periplasmic space. Bar, 20 nm. (B) Group 2 pattern included all the banded envelopes (displaying a thick layer in the inner leaflet of the outer membrane) but no internal cytoplasmic membranes. Bar, 20 nm. (C) Group 3 included all envelopes with internal cytoplasmic membranes with or without a band. The profile shown corresponds to a four-membrane envelope, the most commonly observed in this group. Notice the differences in intensity (peak depths) between the two leaflets of each membrane layer. Bar, 50 nm. (D) Micrograph with no accompanying profile showing a section of an envelope with a total of six membranes, including the outer membrane. Bar, 50 nm. (E) Micrograph with no profile showing a bacterial section with a three-membrane envelope. The central compartment labeled P likely corresponds to an enlarged periplasm. Bar, 100 nm. (F) Group 4 profiles included all envelopes with an unresolved inner membrane. Although the scan showed putative peaks for the inner membrane, they were too shallow, indicating that the intensities of the membrane and surrounding plasma were very similar. Bar, 20 nm. (G) Group 5 represents spore-like envelopes with an electron-dense periplasm and a multilayered appearance. The outer membrane remained unresolved. Bar, 20 nm. OL-IM, outer leaflet of the inner membrane; IL-IM, inner leaflet of the inner membrane; OL-OM, outer leaflet of the outer membrane; IL-OM, inner leaflet of the outer membrane; P, periplasm; C, cytoplasm; E, extracellular space.

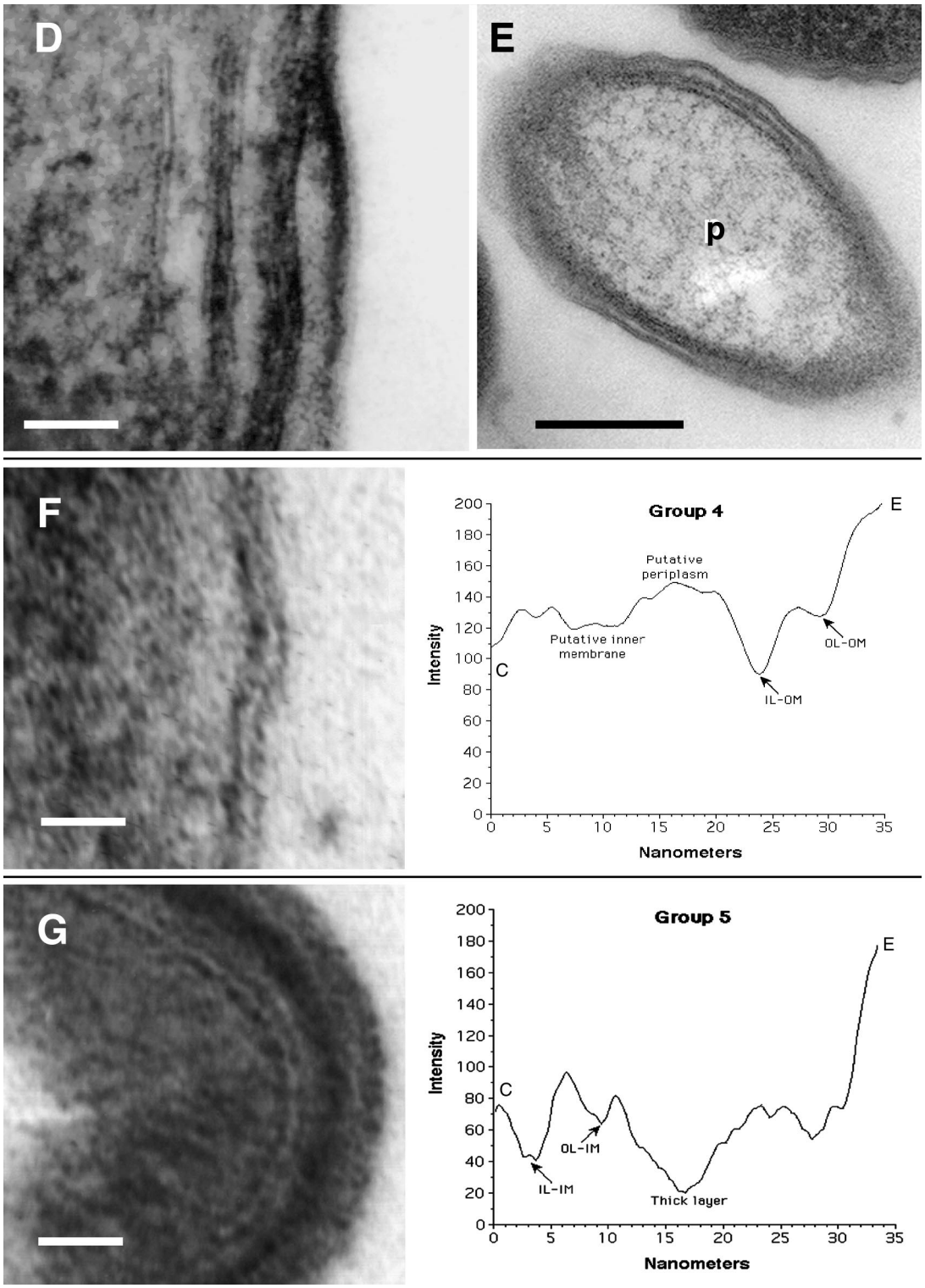


FIG. 8—*Continued*.

grown legionellae displayed spherical cytoplasmic inclusions, virtually every MIF that was fractured across the cytoplasm displayed voluminous inclusions (Fig. 9A and B). Another striking and quite conserved feature of MIFs was their very uneven distribution of intramembranous particles in the inner membrane (Fig. 9A and B). In contrast, inner membranes of agar-grown legionellae displayed evenly distributed intramembranous particles (Fig. 9C).

To attempt the analysis of intermediate forms by freeze fracture, we prepared specimens from early growth on plates

inoculated with MIFs. We were able to confirm the presence of periplasmic vesicles (Fig. 9D), previously shown in thin sections in Fig. 7A and B, implying that these structures cannot be accounted for by processing artifacts alone, as sectioned and fractured specimens were processed and fixed in a fundamentally different way. Importantly, the asymmetric distribution of intramembranous particles in MIFs was lost after growth in vitro, and they appeared homogeneously distributed in most fractures (Fig. 9D).

## DISCUSSION

The notion that *L. pneumophila* differentiates during its intracellular replication in HeLa cells has been advanced previously (26, 27, 29, 38), as has the inappropriateness of the macrophage model to provide an extended time window to study intracellular events or promote legionellar differentiation (27, 29). Our detailed electron microscopy studies now show that *L. pneumophila* follows a stage-specific morphological cycle, closely associated with the occurrence of intracellular events in the host cell. The fact that two unrelated and geographically separated strains of *L. pneumophila* serogroup 1 (Philadelphia-1 and Olda) showed very similar morphological cycles implies that this is a conserved trait of the species. Figure 1 schematically summarizes the developmental stages of *L. pneumophila*, depicting the major morphological forms as we understand them to date. From this, it is clear that this bacterium is highly pleomorphic during its intracellular and extracellular growth cycles.

The total number of legionellar forms identified here was eight. Three forms were identified in vitro: (i) actively replicating, exponential-phase form, (ii) stationary-phase form, and (iii) intermediate form arising when MIFs were placed in BYE broth. The remaining five forms were identified in association with HeLa cells: (iv) early-replicative-phase form, morphologically similar to the exponential-phase replicative form; (v) intermediate, with sharp ripples in the outer membrane emerging in late-replicative-phase vacuoles; (vi) intermediate, with a straight outer membrane and a difficult-to-distinguish inner membrane; (vii) late-replicative-phase intermediate, with a thick layer (with or without inclusions); and (viii) the mature forms arising late in infection (MIFs), with their various envelope configurations and irregular shapes. There were clear morphological similarities between extracellular exponential-phase forms and intracellular early-replicative-phase forms and between stationary-phase forms and some late-replicative-phase intermediates, but their physiological equivalence has not yet been established.

Crucial to the consolidation and reconstruction of the morphological cycle presented here was the identification of intermediates, mostly made possible through observations in vitro (MIF-to-replicative-form transition) or in purified infecting bacteria (replicative form-to-MIF transition). The disadvantage of this approach was that bacterial ultrastructure was examined in the absence of reference markers (defined by the host cell response), which are needed for accurate timing. Nevertheless, it was possible to find in vacuole equivalents of the replicative form-to-MIF transition intermediates, with the exception of forms with fragmented cytoplasm. To our satisfaction, these in vacuole equivalents resided in late-replicative-phase vacuoles, a phase of the cycle that is expected to generate intermediates. It is unclear at this point whether the forms with fragmented cytoplasm were artifacts of the purification process, but even in such a case, it is clear that this particular intermediate responded differently to the sample preparation process, suggesting unique structural differences from the other unfragmented forms.

Numerous reports showing the pleomorphic nature of *L. pneumophila* can now be interpreted in the context of a developmental program. Thus, previously observed morphological variants of *L. pneumophila* (14, 51, 53, 54) and even some (albeit not all) of the bizarre-looking or spore-like forms reported by Katz and Nash (42) could be regarded as differentiated legionellar forms with a defined function. The work of Gress et al. (32) suggests the existence of a developmental cycle in *Legionalla micdadei*. The thick electron-dense layer of the "banded form" of *L. micdadei* (32) is strikingly similar to that present in postreplicative forms (MIFs) of *L. pneumophila*. As we observed with MIFs (27, 29), Gress et al. (32) observed that the banded forms appeared late in infection and did not undergo cell division, as judged by electron microscopy. The "unbanded" morphology of *L. micdadei* (32) was prevalent in agar-grown bacteria and likely equivalent to the *L. pneumophila* replicative forms reported here as having a standard gram-negative morphology.

Many other ultrastructural features observed in this study (and used to identify different forms) have been reported previously. For example, Keel et al. (43) showed legionellar forms with intracytoplasmic membranes and stated that these were extensive in intracellular bacteria. Neblett et al. (50) showed three different legionellar forms, one with a wavy outer membrane (clearly equivalent to the typical replicative form described here) and two intermediate forms with straight outer membranes and an unresolved inner membrane (also reported by Gress et al. [32], Rodgers [53], and Flesher et al. [22]). The fact that the inner membrane could not be visually resolved in the smooth-envelope intermediates does not necessarily mean that these forms were single membraned. Differentiated legionellar forms and intermediates can also be seen in previously published micrographs of infected amoebae (44, 55), showing ultrastructural similarities to the forms presented here.

A consistent observation by investigators who have performed ultrastructural studies with *Legionella* spp. is the absence of a defined peptidoglycan layer, in spite of chemical evidence substantiating its existence (43). In our studies, we also rarely encountered evidence of a peptidoglycan layer. Therefore, it should be very interesting to prove whether the thick electron-dense layer, typical of postreplicative forms, is a thickened peptidoglycan layer, as proposed by Gress et al. (32). The increase in electron density of the periplasm seen in some mature forms, together with the presence of a thick layer of similar density, indeed produced forms with an apparent spore-like laminated envelope. In some cases these forms had irregular shapes and were quite similar to the spore-like forms reported by Katz and Nash (42) (Fig. 5C and 8G). However, the fact that these authors' preparations were contaminated with a gram-positive bacterium that multiplied by septation leaves any possible correlation unresolved.

Although *L. pneumophila* does not form spores in any of its life stages, a legionella-specific monoclonal antibody has been

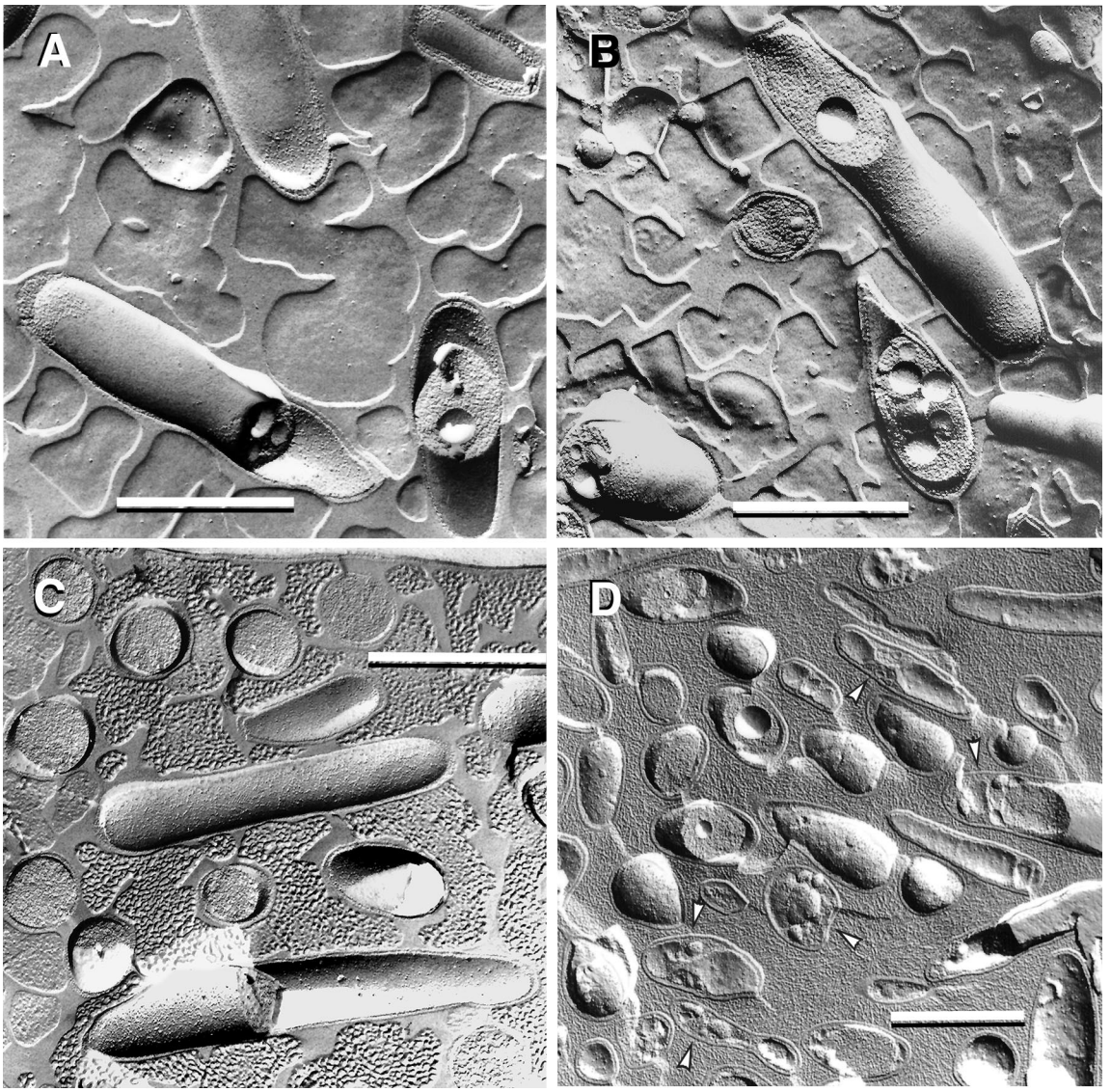


FIG. 9. Freeze fracture analysis of agar-grown and postreplicative SVir forms. (A and B) Fracture replicas of MIFs, showing both cytoplasmic inclusions and an uneven distribution of intramembranous particles in the inner membrane. (C) Fracture replicas of agar-grown bacteria. Notice the lack of inclusions in the exposed fractures across the cytoplasm and the even distribution of intramembranous particles in the inner membrane. (D) Fracture replicas of MIFs after they were grown on BCYE plates to form a visible film. It was common to see small vesicles in areas corresponding to the periplasm (arrowheads) and inner membranes with evenly distributed intramembranous particles. Bars, 1.0 μm.

reported to cross-react with spores but not vegetative cells of the gram-positive bacterium *Bacillus cereus* (23). While difficult to interpret, this observation may indicate that some unusual antigens of *L. pneumophila* may be functionally similar to components of gram-positive spores.

Experimental evidence published elsewhere (27) indicates that stationary-phase forms appear to represent intermediates in the differentiation process to produce MIFs. The presence of multimembranous envelopes (apparently formed as a result of invaginations of the inner membrane) in stationary-phase *L. pneumophila* suggests that this trait is acquired early in the maturation process. In fact, we interpreted the presence of multimembranous envelopes in late-replicative-phase forms (Fig. 4E) as a definite sign of early maturation and reasoned that this feature implies an active synthesis of membrane lipids. The asymmetric distribution (polarization) of intramembranous particles in MIFs and the relative changes in electron density in different components of their complex envelope further suggested an important metabolic conversion. If the host cell exclusively provides the metabolites required to effect these changes, this would partially explain why *L. pneumophila* cannot complete its differentiation in vitro. In this respect, our current documentation of defined morphological changes, presented here as evidence for a developmental cycle in *L. pneumophila*, has marked a pathway to be followed by physiological, biochemical, and genetic studies aimed at reconstructing the molecular process of differentiation and identifying the genes (4) that orchestrate it.

## ACKNOWLEDGMENTS

The thorough technical assistance of Mary Anne Trevors is gratefully acknowledged, as is the participation of Avery Goodwin in the microscopy of the in vitro intermediates. We also thank the anonymous reviewers for excellent suggestions to improve our manuscript.

The Natural Sciences and Engineering Research Council of Canada and the Canadian Institutes of Health Research (grant MT14443) provided funding for this project.

## REFERENCES

1. **Abu Kwaik, Y.** 1996. The phagosome containing *Legionella pneumophila* within the protozoan *Hartmanella vermiformis* is surrounded by the rough endoplasmic reticulum. Appl. Environ. Microbiol. **62:**2022–2028.
2. **Abu Kwaik, Y., B. I. Eisenstein, and N. C. Engleberg.** 1993. Phenotypic modulation by *Legionella pneumophila* upon infection of macrophages. Infect. Immun. **61:**1320–1329.
3. **Abu Kwaik, Y., L.-Y. Gao, B. J. Stone, C. Venkataraman, and O. S. Harb.** 1998. Invasion of protozoa by *Legionella pneumophila* and its role in bacterial ecology and pathogenesis. Appl. Environ. Microbiol. **64:**3127–3133.
4. **Abu Kwaik, Y., and L. L. Pederson.** 1996. The use of differential display-PCR to isolate and characterize a *Legionella pneumophila* locus induced during the intracellular infection of macrophages. Mol. Microbiol. **21:**543–556.
5. **Alli, O. A. T., L.-Y. Gao, L. L. Pedersen, S. Zink, M. Radulic, M. Doric, and Y. Abu Kwaik.** 2000. Temporal pore formation-mediated egress from macrophages and alveolar epithelial cells by *Legionella pneumophila.* Infect. Immun. **68:**6431–6440.
6. **Andrews, H. L., J. P. Vogel, and R. R. Isberg.** 1998. Identification of linked *Legionella pneumophila* genes essential for intracellular growth and evasion of the endocytic pathway. Infect. Immun. **66:**950–958.
7. **Barker, J., P. A. Lambert, and M. R. W. Brown.** 1993. Influence of intra-amoebic and other growth conditions on the surface properties of *Legionella pneumophila*. Infect. Immun. **61:**3503–3510.
8. **Berger, K. H., J. J. Merriam, and R. R. Isberg.** 1994. Altered intracellular targeting properties associated with mutations in the *Legionella pneumophila dotA* gene. Mol. Microbiol. **14:**809–822.
9. **Berk, S. G., R. S. Ting, G. W. Turner, and R. J. Ashburn.** 1998. Production of respirable vesicles containing live *Legionella pneumophila* cells by two *Acanthamoeba* spp. Appl. Environ. Microbiol. **64:**279–286.
10. **Bozue, J. A., and W. Johnson.** 1996. Interaction of *Legionella pneumophila* with *Acanthamoeba castellanii*: uptake by coiling phagocytosis and inhibition of phagosome-lysosome fusion. Infect. Immun. **64:**668–673.
11. **Brand, B. C., A. B. Sadosky, and H. A. Shuman.** 1994. The *Legionella pneumophila icm* locus: a set of genes required for intracellular multiplication in human macrophages. Mol. Microbiol. **14:**797–808.
12. **Brieland, J., J. C. Fantone, D. G. Remick, M. LeGendre, M. McClain, and C. Engleberg.** 1997. The role of *Legionella pneumophila*-infected *Hartmanella vermiformis* as an infectious particle in a murine model of Legionnaires' disease. Infect. Immun. **65:**5330–5333.
13. **Byrne, B., and M. S. Swanson.** 1998. Expression of *Legionella pneumophila* virulence traits in response to growth conditions. Infect. Immun. **66:**3029–3034.
14. **Chandler, F. W., R. M. Cole, M. D. Hicklin, J. A. Blackmon, and C. S. Callaway.** 1979. Ultrastructure of the Legionnaires' disease bacterium—a study using transmission electron microscopy. Ann. Intern. Med. **90:**642–647.
15. **Cirillo, J. D., S. L. G. Cirillo, L. Yan, L. E. Bermudez, S. Falkow, and L. S. Tompkins.** 1999. Intracellular growth in *Acanthamoeba castellani* affects monocyte entry mechanisms and enhances virulence of *Legionella pneumophila*. Infect. Immun. **67:**4427–4434.
16. **Cirillo, J. D., S. Falkow, and L. S. Tompkins.** 1994. Growth of *Legionella pneumophila* in *Acanthamoeba castellani* enhances invasion. Infect. Immun. **62:**3254–3261.
17. **Clemens, D. L., B.-Y. Lee, and M. A. Horwitz.** 2000. Deviant expression of Rab5 on phagosomes containing the intracellular pathogens *Mycobacterium tuberculosis* and *Legionella pneumophila* is associated with altered phagosomal fate. Infect. Immun. **68:**2671–2684.
18. **Fernandez, R. C., S. H. S. Lee, D. Haldane, R. Sumarah, and K. R. Rozee.** 1989. Plaque assay for virulent *Legionella pneumophila*. J. Clin. Microbiol. **27:**1961–1964.
19. **Fernandez, R. C., S. M. Logan, S. H. S. Lee, and P. S. Hoffman.** 1996. Elevated levels of *Legionella pneumophila* stress protein Hsp60 early in infection of human monocytes and L929 cells correlate with virulence. Infect. Immun. **64:**1968–1976.
20. **Fields, B. S.** 1993. *Legionella* and protozoa: interaction of a pathogen and its natural host, p. 129–136. *In* J. M. Barbaree, R. F. Breiman, and A. P. Dufour (ed.), *Legionella*: current status and emerging perspectives. American Society for Microbiology, Washington, D.C.
21. **Fields, B. S.** 1996. The molecular ecology of legionellae. Trends Microbiol. **4:**286–290.
22. **Flesher, A. R., S. Ito, B. J. Mansheim, and D. L. Kasper.** 1979. The cell envelope of the Legionnaires' disease bacterium—morphologic and biochemical characteristics. Ann. Intern. Med. **90:**628–630.
23. **Flournoy, D. J., K. A. Belobraydic, S. L. Silberg, C. H. Lawrence, and P. J. Guthrie.** 1988. False-positive *Legionella pneumophila* direct immunofluorescent monoclonal antibody test caused by *Bacillus cereus* spores. Diagn. Microbiol. Infect. Dis. **9:**123–125.
24. **Gao, L. Y., and Y. Abu Kwaik.** 2000. The mechanism of killing and exiting the protozoan host *Acanthamoeba polyphaga* by *Legionella pneumophila*. Environ. Microbiol. **2:**79–90.
25. **Garduño, R. A., G. Faulkner, M. A. Trevors, N. Vats, and P. S. Hoffman.** 1998. Immunolocalization of Hsp60 in *Legionella pneumophila*. J. Bacteriol. **180:**505–513.
26. **Garduño, R. A., E. Garduño, M. Hiltz, D. Allan, and P. S. Hoffman.** 2001. Morphological and physiological evidence for a developmental cycle in *Legionella pneumophila*, p. 82–85. *In* R. Marre, Y. Abu Kwaik, C. Bartlett, N. P. Cianciotto, B. S. Fields, M. Frosch, J. Hacker, and P. C. Lück (ed.), *Legionella*. ASM Press, Washington, D.C.
27. **Garduño, R. A., E. Garduño, M. F. Hiltz, and P. S. Hoffman.** 2002. Intracellular growth of *Legionella pneumophila* gives rise to a differentiated form dissimilar to stationary-phase forms. Infect. Immun. **70:**6273-6283.
28. **Garduño, R. A., E. Garduño, and P. S. Hoffman.** 1998. Surface-associated Hsp60 chaperonin of *Legionella pneumophila* mediates invasion in a HeLa cell model. Infect. Immun. **66:**4602–4610.
29. **Garduño, R. A., F. D. Quinn, and P. S. Hoffman.** 1998. HeLa cells as a model to study the invasiveness and biology of *Legionella pneumophila*. Can. J. Microbiol. **44:**430–440.
30. **Goldoni, P., L. Cattani, S. Carrara, M. Castellani-Pastoris, L. Sinibaldi, and N. Orsi.** 1998. Multiplication of *Legionella pneumophila* in HeLa cells in the presence of cytoskeleton and metabolic inhibitors. Microbiol. Immunol. **42:**271–279.
31. **Graham, L. L., and T. J. Beveridge.** 1990. Evaluation of freeze-substitution and conventional embedding protocols for routine electron microscopic processing of eubacteria. J. Bacteriol. **172:**2150–2159.
32. **Gress, F. M., R. L. Myerowitz, A. W. Pascule, C. R. Rinaldo, Jr., and J. N. Dowling.** 1980. The ultrastructural morphologic features of Pittsburgh pneumonia agent. Am. J. Pathol. **101:**63–78.
33. **Hammer, B. K., and M. S. Swanson.** 1999. Coordination of *Legionella pneumophila* virulence with entry into stationary phase by ppGpp. Mol. Microbiol. **33:**721–731.
34. **Hanaichi, T., T. Sato, T. Iwamoto, Y. Malavasi-Yamashiro, M. Hoshino, and N. Mizuno.** 1986. A stable stain by modification of Sato's method. J. Electron Microsc. **35:**304–306.
35. **Hatch, T. P., I. Allan, and J. H. Pearce.** 1984. Structural and polypeptide differences between envelopes of infective and reproductive life cycle forms of *Chlamydia* spp. J. Bacteriol. **157:**13–20.
36. **Heinzen, R. A., T. Hackstadt, and J. E. Samuel.** 1999. Developmental biology of *Coxiella burnetii*. Trends Microbiol. **7:**149–154.
37. **Hoffman, P. S., C. A. Butler, and F. D. Quinn.** 1989. Cloning and temperature-dependent expression in *Escherichia coli* of a *Legionella pneumophila* gene coding for a genus-common 60-kilodalton antigen. Infect. Immun. **58:**1731–1739.
38. **Hoffman, P. S., and R. Garduño.** 1999. Pathogenesis of *Legionella pneumophila* infection, p. 131–147. *In* L. J. Paradise, H. Friedman, and M. Bendinelli (ed.), Opportunistic intracellular bacteria and immunity. Plenum Press, New York, N.Y.
39. **Horwitz, M. A.** 1983. Formation of a novel phagosome by the Legionnaires' disease bacterium (*Legionella pneumophila*) in human monocytes. J. Exp. Med. **158:**1319–1331.
40. **Joshi, A. D., S. Sturgill-Koszycki, and M. S. Swanson.** 2001. Evidence that Dot-dependent and -independent factors isolate the *Legionella pneumophila* phagosome from the endocytic network in mouse macrophages. Cell. Microbiol. **3:**99–114.
41. **Karnovsky, M. J.** 1965. A formaldehyde-glutaraldehyde fixative of high osmolality for use in electron microscopy. J. Cell Biol. **27:**137A-138A.
42. **Katz, S. M., and P. Nash.** 1978. The morphology of the Legionnaires' disease organism. Am. J. Pathol. **90:**701–722.
43. **Keel, J. A., W. R. Finnerty, and J. C. Feeley.** 1979. Fine structure of the Legionnaires' disease bacterium—in vitro and in vivo studies of four isolates. Ann. Intern. Med. **90:**652–655.
44. **Kilvington, S., and J. Price.** 1990. Survival of *Legionella pneumophila* within cysts of *Acanthamoeba polyphaga* following chlorine exposure. J. Appl. Bacteriol. **68:**519–525.
45. **Lee, J. V., and A. A. West.** 1991. Survival and growth of *Legionella* species in the environment. J. Appl. Bacteriol. Symp. Suppl. **70:**121S-129S.
46. **McCaul, T. F., and J. C. Williams.** 1981. Developmental cycle of *Coxiella burnetii*: structure and morphogenesis of vegetative and sporogenic differentiations. J. Bacteriol. **147:**1063–1076.
47. **Molmeret, M., O. A. Alli, S. Zink, A. Flieger, N. P. Cianciotto, and Y. Abu Kwaik.** 2002. IcmT is essential for pore formation-mediated egress of *Legionella pneumophila* from mammalian and protozoan cells. Infect. Immun. **70:**69–78.

48. **Moulder, J. W.** 1991. Interaction of chlamydiae and host cells in vitro. Microbiol. Rev. **55:**143–190.
49. **Moulder, J. W.** 1985. Comparative biology of intracellular parasitism. Microbiol. Rev. **49:**298–337.
50. **Neblett, T. R., J. M. Riddle, and M. Dumoff.** 1979. Surface topography and fine structure of the Legionnaires' disease bacterium—a study of six isolates from hospitalized patients. Ann. Intern. Med. **90:**648–651.
51. **Oldham, L. J., and F. G. Rodgers.** 1985. Adhesion, penetration and intracellular replication of *Legionella pneumophila*: an in vitro model of pathogenesis. J. Gen. Microbiol. **131:**697–706.
52. **Pascule, A. W., J. C. Feeley, R. J. Gibson, L. G. Cordes, R. L. Meyerowitz, C. M. Patton, G. W. German, C. L. Carmack, J. W. Ezzell, and J. N. Dowling.** 1980. Pittsburgh pneumonia agent: direct isolation from human lung tissue. J. Infect. Dis. **141:**727–732.
53. **Rodgers, F. G.** 1979. Ultrastructure of *Legionella pneumophila*. J. Clin. Pathol. **32:**1195–1202.
54. **Rodgers, F. G., A. D. Macrae, and M. J. Lewis.** 1978. Electron microscopy of the organism of Legionnaires' disease. Nature **272:**825–826.
55. **Rowbotham, T. J.** 1986. Current views on the relationships between amoebae, legionellae and man. Isr. J. Med. Sci. **22:**678–689.
56. **Roy, C. R., K. H. Berger, and R. R. lsberg.** 1998. *Legionella pneumophila* DotA protein is required for early phagosome trafficking decisions that occur within minutes of bacterial uptake. Mol. Microbiol. **28:**663–674.
57. **Schachter, J.** 1988. The intracellular life of *Chlamydia*. Curr. Top. Microbiol. Immunol. **138:**109–139.
58. **Schofield, G. M.** 1985. A note on the survival of *Legionella pneumophila* in stagnant tap water. J. Appl. Bacteriol. **59:**333–335.
59. **Segal, G., and H. A. Shuman.** 1999. *Legionella pneumophila* utilizes the same genes to multiply within *Acanthamoeba castellanii* and human macrophages. Infect. Immun. **67:**2117–2124.
60. **Skaliy, D., and H. V. McEachern.** 1979. Survival of the Legionnaires' disease bacterium in water. Ann. Intern. Med. **90:**662–663.
61. **Steinert, M., L. Emödy, R. Amaim, and J. Hacker.** 1997. Resuscitation of viable but nonculturable *Legionella pneumophila* Philadelphia JR32 by *Acanthamoeba castellanii*. Appl. Environ. Microbiol. **63:**2047–2053.
62. **Susa, M., J. Hacker, and R. Marre.** 1996. De novo synthesis of *Legionella pneumophila* antigens during intracellular growth in phagocytic cells. Infect. Immun. **64:**1679–1684.
63. **Swanson, M. S., and R. R. lsberg.** 1995. Association of *Legionella pneumophila* with the macrophage endoplasmic reticulum. Infect. Immun. **63:**3609–3620.
64. **Tilney, L. G., O. S. Harb, P. S. Connelly, C. G. Robinson, and C. R. Roy.** 2001. How the parasitic bacterium *Legionella pneumophila* modifies its phagosome and transforms it into rough ER: implications for conversion of plasma membrane to the ER membrane. J. Cell Sci. **114:**4637–4650.
65. **Watarai, M., H. L. Andrews, and R. R. Isberg.** 2001. Formation of a fibrous structure of *Legionella pneumophila* associated with exposure of DotH and DotO proteins after intracellular growth. Mol. Microbiol. **39:**313–329.